



Age-Dependent Glycomic Response to the 2009 Pandemic H1N1 Influenza Virus and Its Association with Disease Severity

Shuhui Chen, Brian Kasper, Bin Zhang, Lauren P. Lashua, Ted M. Ross, Elodie Ghedin, and Lara K. Mahal*



Cite This: *J. Proteome Res.* 2020, 19, 4486–4495



Read Online

ACCESS |



Metrics & More



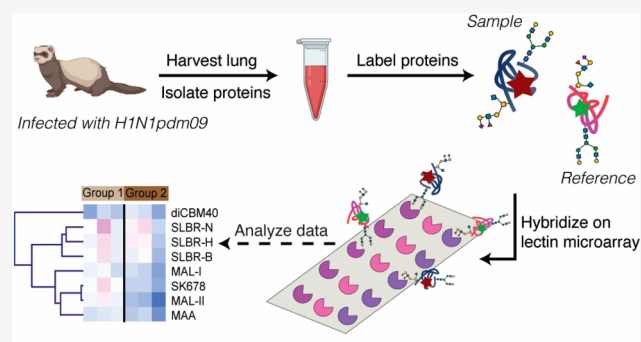
Article Recommendations



Supporting Information

ABSTRACT: Influenza A viruses cause a spectrum of responses, from mild coldlike symptoms to severe respiratory illness and death. Intrinsic host factors, such as age, can influence disease severity. Glycosylation plays a critical role in influenza pathogenesis; however, the molecular drivers of influenza outcomes remain unknown. In this work, we characterized the host glycomic response to the H1N1 2009 pandemic influenza A virus (H1N1pdm09) as a function of age-dependent severity in a ferret model. Using our dual-color lectin microarray technology, we examined baseline glycosylation and glycomic response to infection in newly weaned and aged animals, models for young children and the elderly, respectively. Compared to adult uninfected ferrets, we observed higher levels of α -2,6-sialosides, the receptor for H1N1pdm09, in newly weaned and aged animals. We also observed age-dependent loss of O-linked α -2,3-sialosides. The loss of these highly charged groups may impact viral clearance by mucins, which corresponds to the lower clearance rates observed in aged animals. Upon infection, we observed dramatic changes in the glycomes of aged animals, a population severely impacted by the virus. In contrast, no significant alterations were observed in the newly weaned animals, which show mild to moderate responses to the H1N1pdm09. High mannose, a glycan recently identified as a marker of severity in adult animals, increased with severity in the aged population. However, the response was delayed, in line with the delayed development of pneumonia observed. Overall, our results may help explain the differential susceptibility to influenza A infection and severity observed as a function of age.

KEYWORDS: lectin array, lectin microarray, glycomics, influenza, high mannose, H1N1



INTRODUCTION

Influenza A viruses cause a spectrum of responses from mild coldlike symptoms to severe respiratory illness and death.¹ Both viral strain and intrinsic host factors, such as age, influence disease severity.² In general, infants, young children, and individuals older than 65 are more likely to have severe clinical outcomes upon influenza infection. However, during pandemic outbreaks, influenza viral strains can emerge that shift the age-dependent infection patterns. In 2009, a novel H1N1 influenza strain (H1N1pdm09) arose that caused severe clinical symptoms more frequently in older children and adults than in young children and the elderly.³ Although the lower severity observed in young children is not clearly understood, the loss of severity observed in the elderly population was attributed to pre-existing immunity. Prior waves of seasonal and pandemic influenza strains generated antibodies in the older exposed population that neutralized the H1N1pdm09 virus, generating a more productive existing immunity, which lessened severity.

The ferret model of influenza mimics clinical outcomes for the H1N1pdm09 across the age spectrum.^{4–6} Ferrets are an

attractive animal model for influenza, as they share similar lung physiology to humans and recapitulate the pathology observed in clinical populations. In addition, human influenza viruses efficiently replicate in ferrets without the need for adaptation, enabling study of the original viral strains.⁷ This is because ferrets contain the receptor for human influenza, α -2,6-sialic acids, in their upper respiratory tracts. The similarities between the glycans in the respiratory tract of ferrets to those observed in humans make this a good model to study glycomic changes in response to influenza infection.^{8,9}

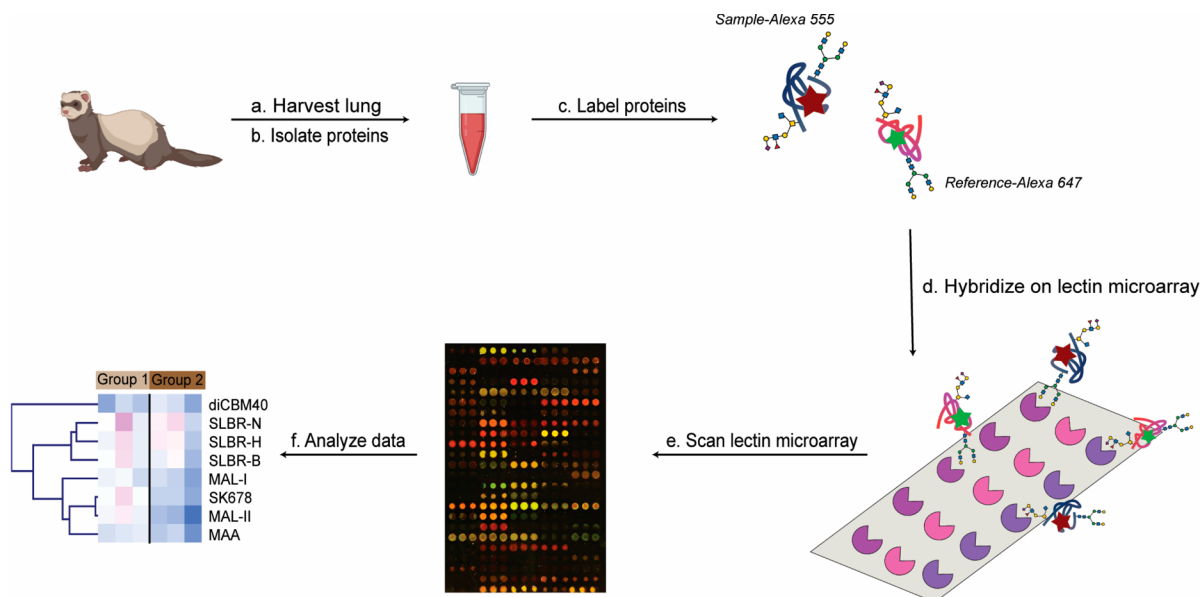
Glycosylation plays an important role in influenza infection and host response.^{10,11} Adhesion of viral hemagglutinin (HA) to host receptors containing terminal α -2,6-sialic acids located in the upper respiratory tract is the first step in the infection

Special Issue: Proteomics in Pandemic Disease

Received: June 22, 2020

Published: September 28, 2020



Scheme 1. Workflow of Sample Preparation for Dual-Color Lectin Microarray Analysis^a

^a(a) Lungs were harvested from ferrets infected with H1N1pdm09 and from uninfected control ferrets. (b) Glycoproteins were isolated from tissues. (c) Glycoproteins were labeled with Alexa Fluor 555-NHS. A pooled reference sample was orthogonally labeled with Alexa Fluor 647-NHS. (d) Equal amounts of sample and reference were mixed and hybridized on lectin microarrays. (e) Lectin microarrays were scanned via a fluorescence slide scanner. (f) Extracted data were analyzed.

process. Release of viral particles requires viral neuraminidases (NA) to cleave sialic acids.¹² This enzyme is the target of current therapeutics against influenza.^{13,14} Because of the importance of HA, NA, and sialic acid in influenza biology, the majority of glycomic analysis has focused on these molecules.

In recent work, our laboratory analyzed the glycomic response to H1N1pdm09 in an adult ferret population using our lectin microarray technology.¹⁵ We found that the severity was not related to sialic acid levels but, rather, correlated with the expression of high mannose N-glycans. Histology on ferret lungs showed high mannose levels corresponded with alveolar severity and was present throughout the tissue on multiple cell types. Infection of human lung epithelia with H1N1pdm09 in cell culture recapitulated the increased high mannose observed in ferrets. This glycan signature was found to be cell surface and was upregulated on both viral and host glycoproteins. Expression of high mannose was shown to be downstream of the unfolded protein response (UPR) pathway, which has been shown to play a role in influenza severity.¹⁶ This glycan motif is the recognition element for a number of innate lectins that activate the immune system. The complement-inducing lectin MBL2, which binds high mannose, has been strongly associated with influenza severity.^{17,18} We have shown direct, high mannose-dependent binding of MBL2 to influenza infected cells. On the basis of our work we hypothesize that high mannose, induced via the UPR pathway, may play a causative role in the damage associated with MBL2 in influenza. It is unknown whether this mechanism might underlie age-related differences in severity.

In this work, we examine glycomic changes, including high mannose, upon infection with the pandemic 2009 H1N1 strain of influenza in ferret models of young children and the elderly. Since their introduction in 2005,¹⁹ lectin microarrays have been used to perform glycomic analysis on a wide variety of

samples from microvesicles²⁰ to human tissues.²¹ Herein, we analyze the glycomic response to H1N1pdm09 infection in newly weaned and aged ferrets using our dual-color lectin microarray technology.²² We also compare the baseline glycomes of newly weaned, adult, and aged ferrets. Our data suggest that differences in the glycome, in particular, in the high mannose response, may help explain in part the variation in clinical outcomes as a function of age in influenza infection.

METHODS

Infection of Ferrets with H1N1pdm09

Fitch ferrets (*Mustela putorius furo*, female) were obtained from Triple F Farms (Sayre, PA) and verified as negative for antibodies to circulating influenza A (H1N1 and H3N2) and B viruses. Newly weaned ferrets were defined as 6–7 weeks of age, adult ferrets as 6–12 months of age, and aged ferrets as 5.5–7 years of age. Ferrets were pair-housed in stainless steel cages (Shor-Line) containing Sani-Chips laboratory animal bedding (P.J. Murphy Forest Products) and provided with food and fresh water ad libitum. Newly weaned and adult ferrets were administered intranasally the H1N1pdm09 virus, A/California/07/2009 (Influenza Reagents Resources (IRR), BEI Resources, the Centers for Disease Control and Prevention) at a dose of 10^6 PFU. Aged ferrets were infected at a dose of 10^5 PFU. The animals were monitored daily for weight loss and disease symptoms, including elevated temperature, low activity level, sneezing, and nasal discharge. Animals were randomly assigned to be sacrificed at day 1, 3, 5, 8, or 14 postinfection (DPI) or euthanized if their clinical condition (e.g., loss of >20% body weight) required it.

Tissue Collection

Necropsies were performed to collect lung tissue. Lungs were rinsed with cold phosphate-buffered solution (PBS), and the

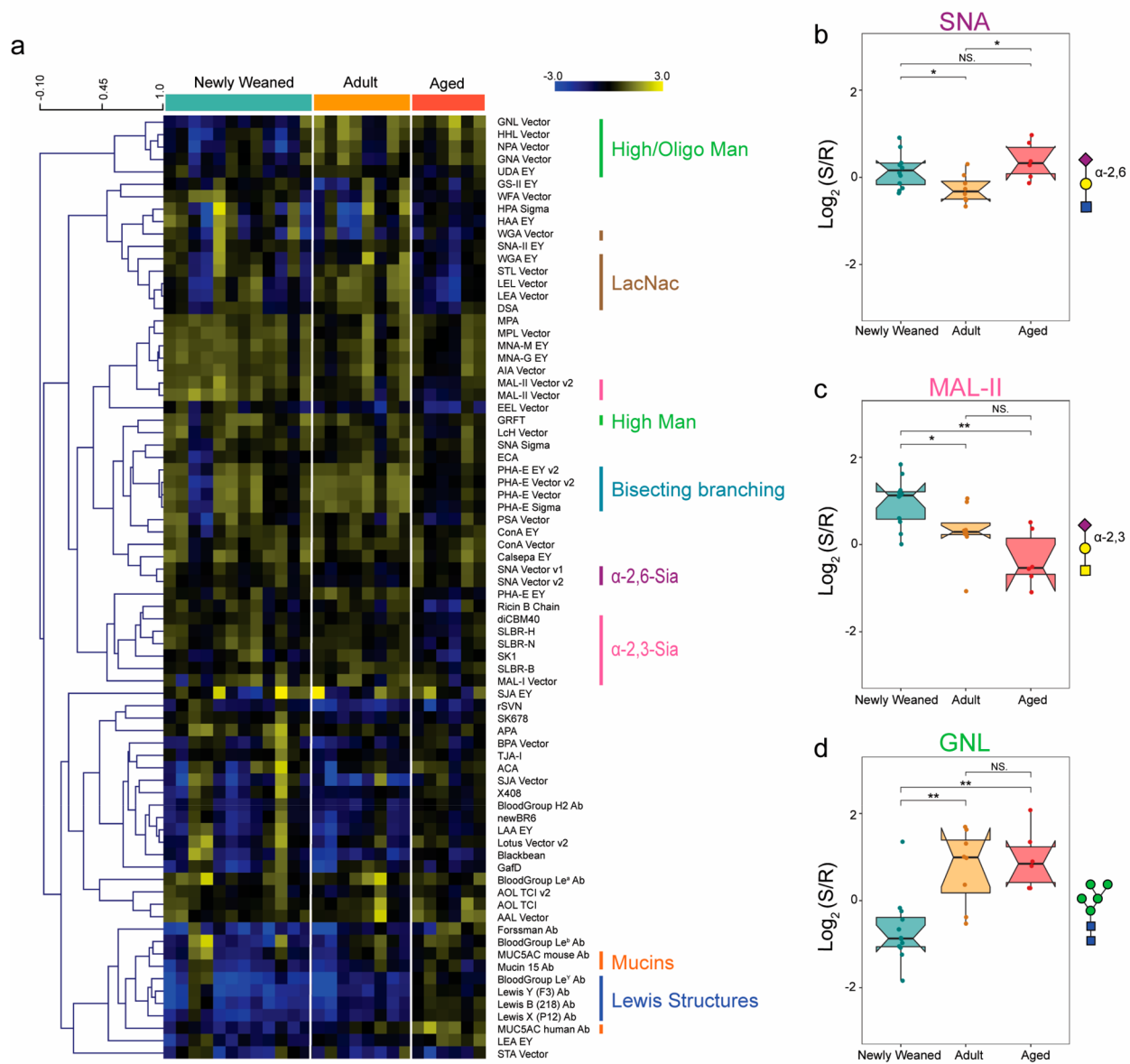


Figure 1. Baseline comparisons between different age groups of uninfected ferrets. (a) Heat map of lectin microarray data. Median normalized \log_2 ratios (Sample (S)/Reference (R)) of ferret lung samples were ordered by age (Newly weaned, $n = 6$, two samples per ferret; Adult, $n = 4$, two samples per ferret; Aged, $n = 3$, 2 samples per ferret). Yellow, $\log_2(S) > \log_2(R)$; blue, $\log_2(R) > \log_2(S)$. Lectins binding α -2,3-sialosides (α -2,3-Sia, pink), α -2,6-sialosides (α -2,6-Sia, purple), high/oligo-mannose (high/oligo-Man, green), bisecting branching (turquoise), *N*-acetyl-*D*-lactosamine (LacNac, brown), mucins (orange) and Lewis structures (blue) are highlighted to the right of the heatmap. (b) Boxplot analysis of lectin binding by SNA (α -2,6-sialosides). (c) Boxplot analysis of lectin binding by MAL-II (α -2,3-sialosides). (d) Boxplot analysis of lectin binding by GNL (oligo-mannose) as a function of age. Newly weaned: cyan; Adult: orange; Aged: red. NS.: Not statistical; (*) $p < 0.05$; (**) $p < 0.01$; (***) $p < 0.001$. Wilcoxon's *t*-test. Glycans bound by lectins are shown in the Symbolic Nomenclature for Glycomics (SNFG) at the side of the boxplots. Symbols are defined as follows: galactose (yellow ●), *N*-acetylgalactosamine (yellow ■), *N*-acetylglucosamine (blue ■), mannose (green ●), sialic acid (purple ◆).

right upper and lower lung lobes were removed. Each lobe was sectioned into quadrants and snap frozen prior to preparation for lectin microarray analysis.

Definition of Severity Metrics

The severity of the infection was determined for all animals studied who were sacrificed at day 8 postinfection. We analyzed two different metrics: weight loss and pneumonia composite score (PCS). In both cases, we determined the cutoffs for mild, moderate, and severe by quartile, wherein mild = Q0-Q1, moderate = Q1-Q3, and severe = Q3-Q4. Weight loss cutoffs for adult ferrets: mild (weight loss <10.8%),

moderate (weight loss: 10.8%–16.5%), and severe (weight loss >16.5%). Cutoffs for aged ferrets: mild (weight loss <18.3%), moderate (weight loss: 18.3%–21.9%), and severe (weight loss >21.9%). PCS cutoffs for newly weaned ferrets: mild (PCS < 8.5), moderate (PCS: 8.5–10.5), and severe (PCS > 10.5). For adult ferrets: mild (PCS < 8), moderate (PCS: 8–10), and severe (PCS > 10). For aged ferrets: mild (PCS < 8.5), moderate (PCS: 8.5–11), and severe (PCS > 11).

Lectin Microarray

Ferret lung tissue samples were washed with PBS supplemented with protease inhibitors cocktails (PIC) and sonicated

on ice in PBS with PIC until completely homogeneous. The homogenized samples were then labeled with Alexa Fluor 555-NHS as previously described.²³ The reference sample was prepared by mixing equal amounts (by total protein) of all samples and labeling with Alexa Fluor 647-NHS (Thermo Fisher). Supporting Information, Table S1, summarizes the print list for each experiment. Printing, hybridization, and data analysis were performed as previously described²⁴ (summarized in the Supporting Information, Table S2).

Data Availability

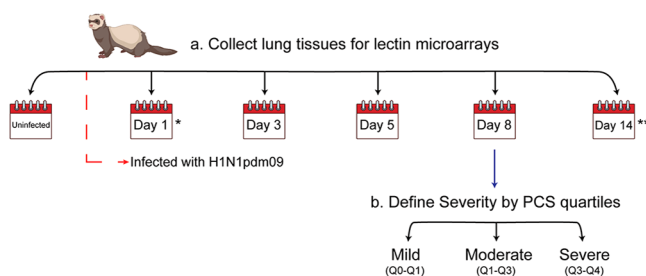
Data are available at DOI: 10.7303/syn22176606.

RESULTS AND DISCUSSION

Ferret Lung Glycosylation Alters with Age

Clinical outcomes and susceptibility to influenza infection vary with age.^{25,26} Given the role host glycans play in influenza

Scheme 2. Workflow of Lung Tissues for Time-Course Study and Severity Analysis^a



^a(a) Lung tissues for aged and newly weaned ferrets were collected. Lung tissues were harvested at different time points post-infection with H1N1pdm09 for lectin microarray analysis. (*) Day 1 time point was not collected for newly weaned ferrets. (**) Aged animals were sacrificed at day 8 due to weight loss greater than 20%. (b) Severity was defined by PCS quartiles for each age group at day 8 post-infections.

infection and in the immune response, we characterized the baseline glycosylation in the lungs of uninfected female ferrets from three age categories: newly weaned, adult, and aged. Newly weaned ferrets were defined as those from six to seven weeks of age. The course of H1N1pdm09 infection in this ferret population mirrors that observed clinically in young children, that is, a mild to moderate presentation of symptoms.⁵ Adult ferrets, defined as 6–12 months of age, have more varied responses to H1N1pdm09 infection ranging from mild to severe, again in line with human populations.⁴ In aged ferrets, defined as 5.5–7 years of age, severe outcomes are seen in more than 50% of animals infected with H1N1pdm09.⁶ This is in line with the higher severity seen in aged populations from influenza A infections in general.^{29,30} However, it does not match clinical observations in the aged human population for the H1N1pdm09 strain. This difference is accounted for by pre-existing immunity in the aged human population. Infection by earlier pandemic-like H1N1 viruses is thought to have elicited cross-reactive antibodies that neutralized the virus, moderating the severity of H1N1pdm09 in the older population.^{27,28} In contrast, the aged ferrets in our study are a naive population with no pre-exposure to influenza. Thus, we observe the more severe influenza response typical of influenza A infections in the elderly with no preimmunity.

We analyzed the baseline expression level of host glycans prior to influenza virus infection in lung punch biopsies from newly weaned (NW, $n = 6$), adult (AD, $n = 4$), and aged ferrets (AG, $n = 3$) using our dual-color lectin microarray technology (Scheme 1).^{22,23} Biopsies from both the upper and lower lobes were analyzed for each ferret. Lectin microarrays utilize carbohydrate-binding proteins with well-defined specificities to detect glycan changes between samples.^{19,22–24} In brief, frozen tissue samples were sonicated and labeled with either Alexa Fluor 555-NHS (sample) or Alexa Fluor 647-NHS (reference). A pooled reference consisting of all the samples was used. Equal amounts of sample and reference were analyzed on the lectin microarrays (>100 probes, Supporting Information, Table S1). A heatmap of the normalized data, ordered by ferret age, is shown in Figure 1a.

Sialic acid glycoconjugates on the host cell surface play a crucial role as both the receptor for influenza binding by hemagglutinin (α -2,6-sialosides) and as the target of the influenza neuraminidase (α -2,3- and α -2,6-sialosides). Differences in sialoside levels may play a role in differential susceptibility to the virus with age. In light of this we examined the expression level of α -2,3- and α -2,6-sialosides in the ferret lung. Both newly weaned and aged ferret lungs had higher levels of α -2,6-sialosides than adult lungs (lectins: SNA, TJA-I, ~1.3-fold NW/AD, ~1.4-fold AG/AD, Figure 1b and Supporting Information, Figure S1), indicating that they may be more susceptible to viral infection. In contrast to α -2,6-sialic acid, we observed a significant age-dependent decrease in α -2,3-sialosides (lectin: MAL-II (~1.5-fold NW/AD, ~2-fold NW/AG), SLBR-N,³¹ diCBM40, SLBR-H,³¹ Figure 1c and Supporting Information, Figure S2). Of particular note, the lectin MAL-II mainly recognizes α -2,3-sialic acids on O-linked glycans. These glycans commonly decorate proteins such as mucins, whose heavily sialylated structures often act as a trap for viral particles.³² While a decrease in α -2,3-sialosides is observed with age, we also observed an increase in mucin levels in the lungs (Antibodies: MUC5AC, MUC15, Supporting Information, Figure S3). In addition, we observed a potentially related increase in Lewis structures (Le), which often decorate mucins (Antibodies: Le^b, Le^x, Le^y, Supporting Information, Figure S4). Taken together, our data suggest that the protective, highly sialylated mucins,^{33–35} which allow clearance of the virus from the lungs, may alter with age in a way that diminishes their protective capacity. These data correlate well with the differences in viral clearance observed in these ferrets, with young ferrets showing more rapid clearance and aged ferrets showing prolonged infection and lower clearance of the virus upon infection.⁶

Recently, our group identified high mannose as a severity marker for influenza H1N1pdm09 infection in adult ferrets.¹⁵ High mannose (defined here as Man_{7–9}) and oligo-mannose (defined as Man_{5–7}) are targets for innate immune lectin binding and may play a direct role in the damage observed in influenza. Analysis of the mannose binding lectins on the array showed distinct profiles for levels of high- and oligo-mannose.³⁶ Uninfected newly weaned animals had significantly lower levels of oligo-mannose (GNL, NPA, HHL) than either adult or aged ferrets (Figure 1d and Supporting Information, Figure S5). However, high-mannose levels, recognized by the antiviral lectin Griffithsin (GRFT),³⁷ were higher in the newly weaned and adult animals as compared to the aged ferrets. Whether age-dependent differences in the baseline levels of

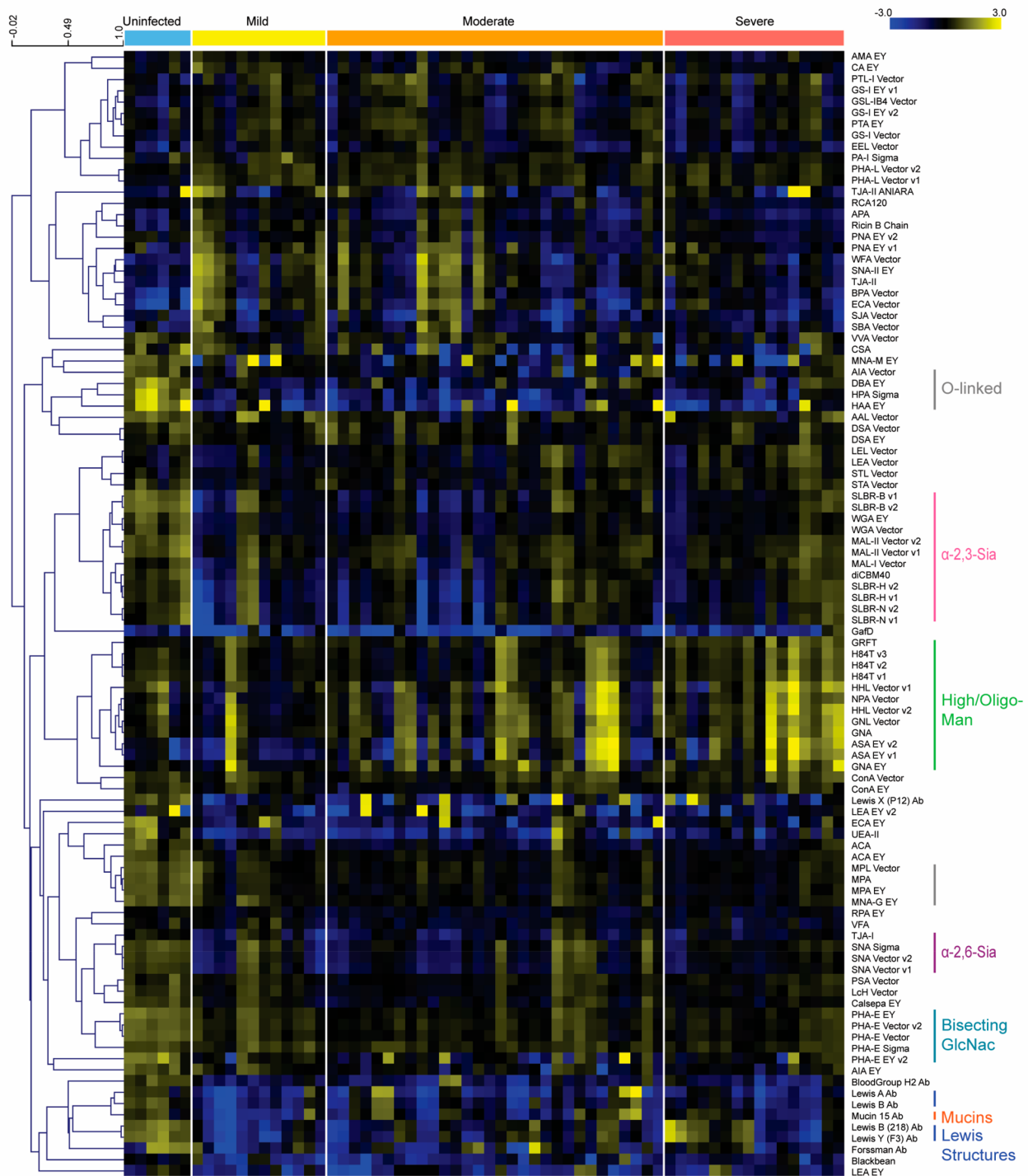


Figure 2. Glycomic changes in aged ferrets in response to influenza infection. Heat map of lectin microarray data for aged ferrets (>5.5 years) infected with H1N1pdm09. Median normalized log₂ ratios (Sample (S))/Reference(R)) of ferret lung samples were ordered by severity. Uninfected (blue): $n = 3$. DPI 8: Mild (yellow), $n = 6$; Moderate (orange), $n = 15$; Severe (red), $n = 8$. Two samples per ferret. Yellow, log₂(S) > log₂(R); Blue, log₂(R) > log₂(S). Lectins binding α-2,3-sialosides (pink), α-2,6-sialosides (purple), high/oligo-mannose (green), bisecting GlcNac (turquoise), O-linked glycans (charcoal) and Lewis structures (blue) are highlighted to the right of the heat map.

mannose in uninfected animals have any bearing on the levels induced during host response to influenza is currently unclear.

Aged Ferrets Have a Distinct Glycomic Response from Adults to Influenza Infection

Disease progression in adult and aged ferrets infected with H1N1pdm09 differs dramatically in timing and presentation.⁶

Aged ferrets had more persistent viral infections and were unable to clear the virus by day 8 postinfection, in contrast to adults. They also developed pneumonia later in the course of their illness and had higher rates of mortality. To study the impact of glycosylation on the host response to influenza in the aged population, we performed lectin microarray analysis on lung punch biopsies from infected aged ferrets (age >5.5

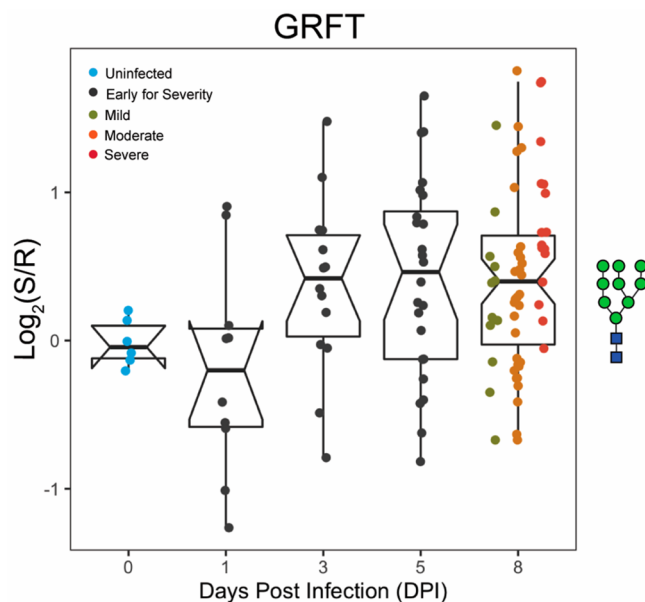


Figure 3. Dynamic changes in high-mannose are observed upon infection in aged ferrets. Time-course analysis of high-mannose as observed by GRFT following H1N1pdm09 infection ($t = 0, 1, 3, 5,$ and 8 d). Boxplot of median normalized \log_2 ratios (Sample (S)/Reference (R)) is shown. Disease severity is indicated by color (Uninfected: blue; Early for Severity: black; Mild: dark yellow; Moderate: orange; Severe: red). Glycans bound by GRFT are shown in the symbolic nomenclature for glycomics at the side of the boxplots.

years). We performed two concurrent studies: a severity study at day 8 postinfection (dpi 8, $n = 29$ ferrets) and a time-course analysis that included the day 8 samples (dpi 1: $n = 5$; dpi 3: $n = 7$; dpi 5: $n = 12$ ferrets, Scheme 2). Uninfected aged ferrets were used as a control ($n = 3$ ferrets). We analyzed two samples for each ferret.

The animals analyzed in this study were the same animals for which pathology data were obtained in Bissel et al.⁶ In our previous work, weight loss was used to evaluate the severity of illness.^{6,15} This is a common metric for severity in animal models and can only be used for time points at more than 5 d postinfection. In studying the disease progression in aged ferrets we observed a disparity between the pathology and the weight loss data. In this age group, a severe outcome by weight loss was defined as greater than 20% loss of mass.⁶ A pneumonia composite score, which sums the scores for lung involvement, bronchial severity, and alveolar severity, was used to evaluate severity by pathology.⁶ In aged animals, which present with pneumonia at later stages of infection, degree of severity by pathology cannot be determined for early time points. A comparison of the severity as defined by weight loss quartiles (Q0-Q1: <18.3%, Q1-Q3: 18.3%–21.9%, Q3-Q4: >21.9%, Supporting Information, Figure S6) to the pneumonia composite scores at day 8 showed no concordance between the two metrics. Instead, in the aged population the trend was toward lower weight loss with increased severity by pathology. This is in direct opposition to the trend observed in adult ferrets. On the basis of our analysis, weight loss was not an appropriate metric for severity in aged ferrets. Thus, the pneumonia composite score was used as the severity metric for this cohort, as it represents the physiologically relevant degree of illness in influenza infection. We used quartiles to define

mild, moderate, and severe infections in the aged population (Mild: PCS < 8.5, $n = 6$ ferrets; Moderate: PCS = 8.5–11, $n = 15$; Severe: PCS > 11, $n = 8$). A heat map of the normalized data for ferrets sacrificed at day 7–8 postinfection arranged by severity is presented in Figure 2. A heat map of the time-course analysis for aged ferrets is shown in the Supporting Information, Figure S7.

We observed several changes in aged ferrets as a function of infection that did not overlay onto severity. For ease of comparison between the aged and adult host responses, we reanalyzed the lectin microarray data from our adult ferret cohort¹⁵ using PCS as the severity metric. In our previous work, adult ferrets showed an increase in α -2,6 sialylation at early infection time points, with levels returning to baseline by day 8 postinfection. In contrast, we see a significant loss of α -2,6 sialylation in the aged ferret lungs with this loss occurring early in the course of infection (SNA, TJA-I, Figure 2 and Supporting Information, Figure S8). We also observe a loss in α -2,3-sialosides by day 8 postinfection in aged animals (SLBR-B, SLBR-H, SLBR-N, diCBM-40, MAL-I, MAL-II, Figure 2 and Supporting Information, Figure S9). A similar loss of α -2,3-sialosides was observed in the adult ferrets. However, in this population, the response was immediate, while in the aged animals a more gradual loss of this glycan was observed. Influenza neuraminidases are known to prefer α -2,3-sialosides,^{38,39} and the more gradual loss of this glycan in aged ferrets maps onto the pattern of delayed infection observed in the lungs.⁶

Uninfected aged animals had higher levels of nonsialylated mucins compared to adults. Upon infection, we observed a substantial loss of O-linked glycans, Lewis structures, and mucins in aged ferrets (AIA, HAA, HPA, MPA, MNA-G, Mucin 15, Le^a, Le^b, Le^y, Figure 2 and Supporting Information, Figure S10). This is similar to previous observations made in adult ferrets; however, the degree of response in the aged ferrets was more pronounced. We observed a strong loss of O-linked glycans, Lewis structures, and mucins at the earliest time points (Supporting Information, Figure S11), which may contribute to the inability of older animals to effectively fight infection.

Our recent work strongly suggests a role for high/oligo-mannose as a key mediator of influenza severity.¹⁵ In our original analysis, the severity in the adult ferrets was defined by weight loss. Reanalysis of these data using pneumonia composite scores did not change the previously observed relationship between the high/oligo-mannose levels and severity (Supporting Information, Figure S12). We observe a similar increase in high mannose as a function of severity in the aged animals when severity is defined by pathology (GRFT, HHL, H84T,⁴⁰ NPA, GNA, ASA, Figure 2, Figure 3, and Supporting Information, Figure S12). However, the timing of high mannose induction in the aged ferrets is delayed when compared to adults. In the adult ferrets, high mannose was induced at day 1 postinfection in line with the damage observed by pathology.⁶ In the aged ferrets, we observe significant changes in high mannose by day 3, which persisted to day 8 postinfection. This is consistent with the more delayed development of pneumonia in these animals. Overall, these data support high mannose as a marker and potential mediator of severity in the host response to influenza infection.

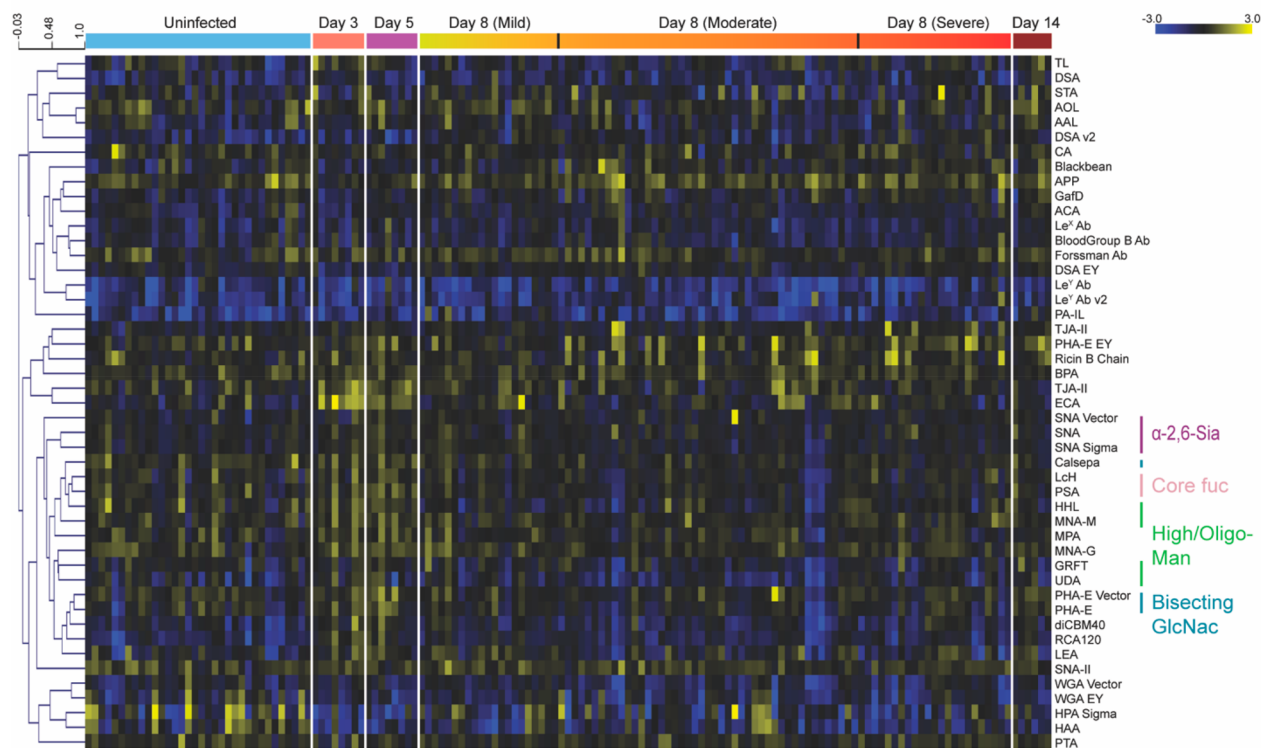


Figure 4. Newly weaned ferrets undergo glycan changes early in response to influenza. Median normalized \log_2 ratios (Sample (S)/Reference(R)) of newly weaned (six to seven weeks of age) ferret lung samples were ordered by days post infection. Uninfected (blue), $n = 16$, two samples per ferret; day 3 (salmon), $n = 4$, two samples per ferret; day 5 (magenta), $n = 4$, two samples per ferret; day 8, ordered by severity (mild, yellow; moderate, orange; severe, red), $n = 42$, two samples per ferret; day 14 (maroon), $n = 3$, two samples per ferret. Yellow, $\log_2(S) > \log_2(R)$; blue, $\log_2(R) > \log_2(S)$. Lectins binding α -2,6-sialosides (purple), high/oligo-mannose (green), bisecting GlcNac (turquoise), and core fucose (light pink) are highlighted to the right of the heatmap.

Newly Weaned Ferrets Show No Severity-Dependent Changes in the Glycome

The 2019 pandemic H1N1 virus presented with mild clinical symptoms in young children.^{41–43} H1N1pdm09 infection in newly weaned ferrets mimic these clinical symptoms, with lower fevers and less weight loss.⁵ Newly weaned ferrets clear the virus faster and have much lower levels of alveolar pneumonia.⁶ We analyzed the glycosylation changes in the lungs of newly weaned ferrets (six to seven weeks) infected with H1N1pdm09, for which we had previously obtained pathology data.⁶ To examine the changes in glycosylation over the course of the infection, we performed a time-course study (uninfected, $n = 16$; dpi 3, $n = 4$; dpi 5, $n = 4$; dpi 8, $n = 42$; dpi 14, $n = 3$, two samples per ferret). Severity was determined for day 8 samples using the PCS metric as previously described. A heat map of the time-course data, organized by severity for day 8 postinfection, is shown in Figure 4.

In contrast to both adults and aged ferrets, we saw no clear severity-dependent differences in the newly weaned animals at day 8 postinfection. We did observe an increase in complex N-glycan epitopes early in the course of infection, peaking by day 5 and returning to preinfection levels by day 8 (α -2,6-sialic acid: SNA; core fucose: LcH, PSA; bisecting branching: PHA-E, Calsepa, Figure 4 and Supporting Information, Figure S13). Although high/oligo-mannose trended with complex N-glycans in the time course, the changes were not statistically significant. Overall, the lack of strong changes in the glycome is consistent with the mild nature of illness observed in young ferrets, modeling the human population.

CONCLUSIONS

In 2009, a new pandemic H1N1 influenza A virus emerged and displayed an unusual severity pattern, impacting adults more severely than young children or the elderly. The lower impact on the elderly population, who are typically at high risk for influenza severity, was later determined to be a result of pre-existing immunity. The ferret model of influenza has been found to mimic the differences in age-dependent illness observed in the absence of pre-existing immunity. In this model, there is a gradient of severity with young ferrets showing mild illness and aged ferrets displaying high severity, as would be expected in an influenza-naive aged human population. The origins of this disparity in host response is still unclear. In this work, we show dramatic age-dependent differences in the ferret glycome and host response to influenza that overlay differences observed in severity. These include age-dependent differences in mucin-related epitopes that may explain differences in viral clearance observed between populations. In recent work, we posited that the induction of high mannose due to influenza infection could be causative of severity through overengagement of the innate immune system via lectins, such as MBL2. Our current study shows that high mannose is induced in the aged population, where high levels of severity are observed, but not in newly weaned ferrets, which display a mild phenotype. This is consistent with our current hypothesis and points to the need for further study to determine if the glycomic host response is a critical mediator of influenza severity.

■ ASSOCIATED CONTENT**SI Supporting Information**

The Supporting Information is available free of charge at <https://pubs.acs.org/doi/10.1021/acs.jproteome.0c00455>.

Boxplots of α -2,6-sialoside signal by age in uninfected ferrets. Boxplots of α -2,3-sialoside levels by age in uninfected ferrets. Boxplots of mucins expressions by age in uninfected ferrets. Boxplots of Lewis structures by age in uninfected ferrets. Boxplots of high/oligo-mannose levels by age in uninfected ferrets. Boxplots of Pneumonia Composite Score (PCS) as a function of weight loss quartiles in adult and aged ferrets. Aged ferrets had delayed response to influenza infection. Impact of influenza infection on α -2,6-sialosides in adult and aged ferrets. Impact of influenza infection on α -2,3-sialosides in adult and aged ferrets. Impact of influenza infection on O-linked glycans in aged ferrets. Dynamic changes in O-linked glycans are observed upon infection in aged ferrets. Comparison of severity metrics used in adult and aged ferrets. Glycan changes are observed early in the time-course study of newly weaned ferrets. Lectins used in microarrays. Lectin microarray information-MIRAGE format (PDF)

■ AUTHOR INFORMATION**Corresponding Author**

Lara K. Mahal – Biomedical Research Institute, Department of Chemistry, New York University, New York, New York 10003, United States; Department of Chemistry, University of Alberta, Edmonton, AB T6G 2G2, Canada; orcid.org/0000-0003-4791-8524; Phone: 780-492-5847; Email: lkmahal@ualberta.ca

Authors

Shuhui Chen – Biomedical Research Institute, Department of Chemistry, New York University, New York, New York 10003, United States

Brian Kasper – Biomedical Research Institute, Department of Chemistry, New York University, New York, New York 10003, United States

Bin Zhang – Department of Genetics and Genomic Sciences, Mount Sinai Center for Transformative Disease Modeling, Icahn Institute of Genomics and Multiscale Biology, Icahn School of Medicine at Mount Sinai, New York, New York 10029, United States

Lauren P. Lashua – Center for Genomics & Systems Biology, Department of Biology, New York University, New York, New York 10003, United States

Ted M. Ross – Center for Vaccines and Immunology, University of Georgia, Athens, Georgia 30602, United States

Elodie Ghedin – Center for Genomics & Systems Biology, Department of Biology, New York University, New York, New York 10003, United States; Systems Genomics Section, Laboratory of Parasitic Diseases, NIAID/NIH, Bethesda, Maryland 20894, United States

Complete contact information is available at:

<https://pubs.acs.org/doi/10.1021/acs.jproteome.0c00455>

Notes

The authors declare no competing financial interest.

■ ACKNOWLEDGMENTS

The University of Georgia Institutional Animal Care and Use Committee approved all experiments under the Animal Use Protocol No. 2015-04-007, which were conducted in accordance with the National Research Council's Guide for the Care and Use of Laboratory Animals, The Animal Welfare Act, and the CDC/NIH's Biosafety in Microbiological and Biomedical Laboratories guide. This work was supported by NIAID/NIH U01 AI111598 to E.G., B.Z., and L.M., and in part by the Division of Intramural Research, National Institute of Allergy and Infectious Diseases, National Institutes of Health. Publication of this research was supported, in part, thanks to funding from the Canada Excellence Research Chairs Program (L.M.). The TOC and Schemes ¹ & ² were created, in part, with Biorender.com.

■ REFERENCES

- (1) Iuliano, A. D.; Roguski, K. M.; Chang, H. H.; Muscatello, D. J.; Palekar, R.; Tempia, S.; Cohen, C.; Gran, J. M.; Schanzer, D.; Cowling, B. J.; Wu, P.; Kyncl, J.; Ang, L. W.; Park, M.; Redlberger-Fritz, M.; Yu, H.; Espenhain, L.; Krishnan, A.; Emukule, G.; van Asten, L.; Pereira da Silva, S.; Aungkulanon, S.; Buchholz, U.; Widdowson, M.-A.; Bresee, J. S.; Azziz-Baumgartner, E.; Cheng, P.-Y.; Dawood, F.; Poppa, I.; Olsen, S.; Haber, M.; Jeffers, C.; MacIntyre, C. R.; Newall, A. T.; Wood, J. G.; Kundi, M.; Popow-Kraupp, T.; Ahmed, M.; Rahman, M.; Marinho, F.; Sotomayor Proschle, C. V.; Vergara Mallegas, N.; Luzhao, F.; Sa, L.; Barbosa-Ramírez, J.; Sanchez, D. M.; Gomez, L. A.; Vargas, X. B.; Acosta Herrera, a.; Llanés, M. J.; Fischer, T. K.; Krause, T. G.; Mølbak, K.; Nielsen, J.; Trebbien, R.; Bruno, A.; Ojeda, J.; Ramos, H.; an der Heiden, M.; del Carmen Castillo Signor, L.; Serrano, C. E.; Bhardwaj, R.; Chadha, M.; Narayan, V.; Kosen, S.; Bromberg, M.; Glatman-Freedman, A.; Kaufman, Z.; Arima, Y.; Oishi, K.; Chaves, S.; Nyawanda, B.; Al-Jarallah, R. A.; Kuri-Morales, P. A.; Matus, C. R.; Corona, M. E. J.; Burmaa, A.; Darmaa, O.; Obtel, M.; Cherkaoui, I.; van den Wijngaard, C. C.; van der Hoek, W.; Baker, M.; Bandaranyake, D.; Bissielo, A.; Huang, S.; Lopez, L.; Newbern, C.; Flem, E.; Grøneng, G. M.; Hauge, S.; de Cosío, F. G.; de Moltó, Y.; Castillo, L. M.; Cabello, M. A.; von Horoch, M.; Medina Osis, J.; Machado, A.; Nunes, B.; Rodrigues, A. P.; Rodrigues, E.; Calomfirescu, C.; Lupulescu, E.; Popescu, R.; Popovici, O.; Bogdanovic, D.; Kostic, M.; Lazarevic, K.; Milosevic, Z.; Todorovic, B.; Chen, M.; Cutter, J.; Lee, V.; Lin, R.; Ma, S.; Cohen, A. L.; Treurnicht, F.; Kim, W. J.; Delgado-Sanz, C.; de mateo Ontañón, S.; Larrauri, A.; León, I. L.; Vallejo, F.; Born, R.; Junker, C.; Koch, D.; Chuang, J.-H.; Huang, W.-T.; Kuo, H.-W.; Tsai, Y.-C.; Bundhamcharoen, K.; Chittaganpitch, M.; Green, H. K.; Pebody, R.; Goñi, N.; Chiparelli, H.; Brammer, L.; Mustaqim, D. Estimates of global seasonal influenza-associated respiratory mortality: a modelling study. *Lancet* **2018**, *391* (10127), 1285–1300.
- (2) Medina, R. A.; Garcia-Sastre, A. Influenza A viruses: new research developments. *Nat. Rev. Microbiol.* **2011**, *9* (8), 590–603.
- (3) Chowell, G.; Bertozzi, S. M.; Colchero, M. A.; Lopez-Gatell, H.; Alpuche-Aranda, C.; Hernandez, M.; Miller, M. A. Severe respiratory disease concurrent with the circulation of H1N1 influenza. *N. Engl. J. Med.* **2009**, *361* (7), 674–9.
- (4) Rowe, T.; Leon, A. J.; Crevar, C. J.; Carter, D. M.; Xu, L.; Ran, L.; Fang, Y.; Cameron, C. M.; Cameron, M. J.; Banner, D.; Ng, D. C.; Ran, R.; Weirback, H. K.; Wiley, C. A.; Kelvin, D. J.; Ross, T. M. Modeling host responses in ferrets during A/California/07/2009 influenza infection. *Virology* **2010**, *401* (2), 257–65.
- (5) Huang, S. S.; Banner, D.; Degousee, N.; Leon, A. J.; Xu, L.; Paquette, S. G.; Kanagasabai, T.; Fang, Y.; Rubino, S.; Rubin, B.; Kelvin, D. J.; Kelvin, A. A. Differential pathological and immune responses in newly weaned ferrets are associated with a mild clinical outcome of pandemic 2009 H1N1 infection. *J. Virol* **2012**, *86* (24), 13187–201.

- (6) Bissel, S. J.; Carter, C. E.; Wang, G.; Johnson, S. K.; Lashua, L. P.; Kelvin, A. A.; Wiley, C. A.; Ghedin, E.; Ross, T. M. Age-Related Pathology Associated with H1N1 A/California/07/2009 Influenza Virus Infection. *Am. J. Pathol.* **2019**, *189* (12), 2389–2399.
- (7) Belser, J. A.; Katz, J. M.; Tumpey, T. M. The ferret as a model organism to study influenza A virus infection. *Dis. Models & Mech.* **2011**, *4* (5), 575–9.
- (8) Walther, T.; Karamanska, R.; Chan, R. W.; Chan, M. C.; Jia, N.; Air, G.; Hopton, C.; Wong, M. P.; Dell, A.; Malik Peiris, J. S.; Haslam, S. M.; Nicholls, J. M. Glycomic analysis of human respiratory tract tissues and correlation with influenza virus infection. *PLoS Pathog.* **2013**, *9* (3), e1003223.
- (9) Jia, N.; Barclay, W. S.; Roberts, K.; Yen, H. L.; Chan, R. W.; Lam, A. K.; Air, G.; Peiris, J. S.; Dell, A.; Nicholls, J. M.; Haslam, S. M. Glycomic characterization of respiratory tract tissues of ferrets: implications for its use in influenza virus infection studies. *J. Biol. Chem.* **2014**, *289* (41), 28489–504.
- (10) Nicholls, J. M. The battle between influenza and the innate immune response in the human respiratory tract. *Infect. Chemother.* **2013**, *45* (1), 11–21.
- (11) Jia, N.; Byrd-Leotis, L.; Matsumoto, Y.; Gao, C.; Wein, A. N.; Lobby, J. L.; Kohlmeier, J. E.; Steinhauer, D. A.; Cummings, R. D. The Human Lung Glycome Reveals Novel Glycan Ligands for Influenza A Virus. *Sci. Rep.* **2020**, *10* (1), 5320.
- (12) Cohen, M.; Zhang, X. Q.; Senaati, H. P.; Chen, H. W.; Varki, N. M.; Schooley, R. T.; Gagneux, P. Influenza A penetrates host mucus by cleaving sialic acids with neuraminidase. *Virology*. **2013**, *10* (1), 321.
- (13) Gubareva, L. V.; Kaiser, L.; Hayden, F. G. Influenza virus neuraminidase inhibitors. *Lancet* **2000**, *355* (9206), 827–835.
- (14) Moscona, A. Neuraminidase inhibitors for influenza. *N. Engl. J. Med.* **2005**, *353* (13), 1363–73.
- (15) Heindel, D. W.; Koppolu, S.; Zhang, Y.; Kasper, B.; Meche, L.; Vaiana, C. A.; Bissel, S. J.; Carter, C. E.; Kelvin, A. A.; Elaish, M.; Lopez-Orozco, J.; Zhang, B.; Zhou, B.; Chou, T.-W.; Lashua, L.; Hobman, T. C.; Ross, T. M.; Ghedin, E.; Mahal, L. K. Glycomic analysis of host-response reveals high mannose as a key mediator of influenza severity. *Proc. Natl. Acad. Sci. U. S. A.* **2020**, in Press.
- (16) Hrinčius, E. R.; Liedmann, S.; Finkelstein, D.; Vogel, P.; Ganseboom, S.; Samarasinghe, A. E.; You, D.; Cormier, S. A.; McCullers, J. A. Acute Lung Injury Results from Innate Sensing of Viruses by an ER Stress Pathway. *Cell Rep.* **2015**, *11* (10), 1591–603.
- (17) Zogheib, E.; Nyga, R.; Cornu, M.; Sendid, B.; Monconduit, J.; Jounieaux, V.; Maizel, J.; Segard, C.; Chouaki, T.; Dupont, H. Prospective Observational Study on the Association Between Serum Mannose-Binding Lectin Levels and Severe Outcome in Critically Ill Patients with Pandemic Influenza Type A (H1N1) Infection. *Lung* **2018**, *196* (1), 65–72.
- (18) Ling, M. T.; Tu, W.; Han, Y.; Mao, H.; Chong, W. P.; Guan, J.; Liu, M.; Lam, K. T.; Law, H. K.; Peiris, J. S.; Takahashi, K.; Lau, Y. L. Mannose-binding lectin contributes to deleterious inflammatory response in pandemic H1N1 and avian H9N2 infection. *J. Infect. Dis.* **2012**, *205* (1), 44–53.
- (19) Pilobello, K. T.; Krishnamoorthy, L.; Slawek, D.; Mahal, L. K. Development of a lectin microarray for the rapid analysis of protein glycopatterns. *ChemBioChem* **2005**, *6* (6), 985–9.
- (20) Batista, B. S.; Eng, W. S.; Pilobello, K. T.; Hendricks-Munoz, K. D.; Mahal, L. K. Identification of a conserved glycan signature for microvesicles. *J. Proteome Res.* **2011**, *10* (10), 4624–33.
- (21) Agrawal, P.; Fontanals-Cirera, B.; Sokolova, E.; Jacob, S.; Vaiana, C. A.; Argibay, D.; Davalos, V.; McDermott, M.; Nayak, S.; Darvishian, F.; Castillo, M.; Ueberheide, B.; Osman, I.; Fenyo, D.; Mahal, L. K.; Hernandez, E. A Systems Biology Approach Identifies FUT8 as a Driver of Melanoma Metastasis. *Cancer Cell* **2017**, *31* (6), 804–819.
- (22) Pilobello, K. T.; Slawek, D. E.; Mahal, L. K. A ratiometric lectin microarray approach to analysis of the dynamic mammalian glycome. *Proc. Natl. Acad. Sci. U. S. A.* **2007**, *104* (28), 11534–9.
- (23) Pilobello, K. T.; Agrawal, P.; Rouse, R.; Mahal, L. K. Advances in lectin microarray technology: optimized protocols for piezoelectric print conditions. *Curr. Protoc. Chem. Biol.* **2013**, *5* (1), 1–23.
- (24) Koppolu, S.; Wang, L.; Mathur, A.; Nigam, J. A.; Dezzutti, C. S.; Isaacs, C.; Meyn, L.; Bunge, K. E.; Moncla, B. J.; Hillier, S. L.; Rohan, L. C.; Mahal, L. K. Vaginal Product Formulation Alters the Innate Antiviral Activity and Glycome of Cervicovaginal Fluids with Implications for Viral Susceptibility. *ACS Infect. Dis.* **2018**, *4* (11), 1613–1622.
- (25) Clohisey, S.; Baillie, J. K. Host susceptibility to severe influenza A virus infection. *Crit. Care* **2019**, *23* (303). DOI: 10.1186/s13054-019-2566-7.
- (26) Czaja, C. A.; Miller, L.; Alden, N.; Wald, H. L.; Cummings, C. N.; Rolfes, M. A.; Anderson, E. J.; Bennett, N. M.; Billing, L. M.; Chai, S. J.; Eckel, S.; Mansmann, R.; McMahon, M.; Monroe, M. L.; Mue, A.; Risk, I.; Schaffner, W.; Thomas, A. R.; Yousey-Hindes, K.; Garg, S.; Herlihy, R. K. Age-Related Differences in Hospitalization Rates, Clinical Presentation, and Outcomes Among Older Adults Hospitalized With Influenza-U.S. Influenza Hospitalization Surveillance Network (FluSurv-NET). *Open Forum Infect. Dis.* **2019**, *6* (7), DOI: 10.1093/ofid/ofz225.
- (27) Giles, B. M.; Bissel, S. J.; Craig, J. K.; Dealmeida, D. R.; Wiley, C. A.; Tumpey, T. M.; Ross, T. M. Elicitation of anti-1918 influenza virus immunity early in life prevents morbidity and lower levels of lung infection by 2009 pandemic H1N1 influenza virus in aged mice. *J. Virol.* **2012**, *86* (3), 1500–13.
- (28) Verma, N.; Dimitrova, M.; Carter, D. M.; Crevar, C. J.; Ross, T. M.; Golding, H.; Khurana, S. Influenza virus H1N1pdm09 infections in the young and old: evidence of greater antibody diversity and affinity for the hemagglutinin globular head domain (HA1 Domain) in the elderly than in young adults and children. *J. Virol.* **2012**, *86* (10), 5515–22.
- (29) Zhang, A. J.; To, K. K.; Tse, H.; Chan, K. H.; Guo, K. Y.; Li, C.; Hung, I. F.; Chan, J. F.; Chen, H.; Tam, S.; Yuen, K. Y. High incidence of severe influenza among individuals over 50 years of age. *Clin. Vaccine Immunol.* **2011**, *18* (11), 1918–24.
- (30) Caini, S.; Spreuwenberg, P.; Kuszniarz, G. F.; Rudi, J. M.; Owen, R.; Pennington, K.; Wangchuk, S.; Gyeltshen, S.; Ferreira de Almeida, W. A.; Pessanha Henriques, C. M.; Njouom, R.; Vernet, M. A.; Fauce, R. A.; Andrade, W.; Yu, H.; Feng, L.; Yang, J.; Peng, Z.; Lara, J.; Bruno, A.; de Mora, D.; de Lozano, C.; Zambon, M.; Pebody, R.; Castillo, L.; Clara, A. W.; Matute, M. L.; Kosasih, H.; Nurhayati; Puzelli, S.; Rizzo, C.; Kadjo, H. A.; Daouda, C.; Kiyankbekova, L.; Ospanova, A.; Mott, J. A.; Emukule, G. O.; Heraud, J. M.; Razanajatovo, N. H.; Barakat, A.; El Falaki, F.; Huang, S. Q.; Lopez, L.; Balmaseda, A.; Moreno, B.; Rodrigues, A. P.; Guiomar, R.; Ang, L. W.; Lee, V. J. M.; Venter, M.; Cohen, C.; Badur, S.; Ciblak, M. A.; Mironenko, A.; Holubka, O.; Bresee, J.; Brammer, L.; Hoang, P. V. M.; Le, M. T. Q.; Fleming, D.; Seblain, C. E.; Schellevis, F.; Paget, J.; Global Influenza, B. S. g. Distribution of influenza virus types by age using case-based global surveillance data from twenty-nine countries, 1999–2014. *BMC Infect. Dis.* **2018**, *18* (1), 269.
- (31) Bensing, B. A.; Li, Q.; Park, D.; Lebrilla, C. B.; Sullam, P. M. Streptococcal Siglec-like adhesins recognize different subsets of human plasma glycoproteins: implications for infective endocarditis. *Glycobiology* **2018**, *28* (8), 601–611.
- (32) Ridley, C.; Thornton, D. J. Mucins: the frontline defence of the lung. *Biochem. Soc. Trans.* **2018**, *46* (5), 1099–1106.
- (33) Lillehoj, E. P.; Kato, K.; Lu, W.; Kim, K. C. Cellular and molecular biology of airway mucins. *Int. Rev. Cell Mol. Biol.* **2013**, *303*, 139–202.
- (34) Delaveris, C. S.; Webster, E. R.; Banik, S. M.; Boxer, S. G.; Bertozzi, C. R. Membrane-tethered mucin-like polypeptides sterically inhibit binding and slow fusion kinetics of influenza A virus. *Proc. Natl. Acad. Sci. U. S. A.* **2020**, *117* (23), 12643–12650.
- (35) Zanin, M.; Baviskar, P.; Webster, R.; Webby, R. The Interaction between Respiratory Pathogens and Mucus. *Cell Host Microbe* **2016**, *19* (2), 159–68.

(36) Wong, M. Y.; Chen, K.; Antonopoulos, A.; Kasper, B. T.; Dewal, M. B.; Taylor, R. J.; Whittaker, C. A.; Hein, P. P.; Dell, A.; Genereux, J. C.; Haslam, S. M.; Mahal, L. K.; Shoulders, M. D. XBP1s activation can globally remodel N-glycan structure distribution patterns. *Proc. Natl. Acad. Sci. U. S. A.* **2018**, *115* (43), E10089–E10098.

(37) Mori, T.; O'Keefe, B. R.; Sowder, R. C., 2nd; Bringans, S.; Gardella, R.; Berg, S.; Cochran, P.; Turpin, J. A.; Buckheit, R. W., Jr.; McMahon, J. B.; Boyd, M. R. Isolation and characterization of griffithsin, a novel HIV-inactivating protein, from the red alga *Griffithsia* sp. *J. Biol. Chem.* **2005**, *280* (10), 9345–53.

(38) Air, G. M. Influenza neuraminidase. *Influenza Other Respir. Viruses* **2012**, *6* (4), 245–56.

(39) Gerlach, T.; Kuhling, L.; Uhlendorff, J.; Laukemper, V.; Matrosovich, T.; Czudai-Matwich, V.; Schwalm, F.; Klenk, H. D.; Matrosovich, M. Characterization of the neuraminidase of the H1N1/09 pandemic influenza virus. *Vaccine* **2012**, *30* (51), 7348–52.

(40) Swanson, M. D.; Boudreaux, D. M.; Salmon, L.; Chugh, J.; Winter, H. C.; Meagher, J. L.; Andre, S.; Murphy, P. V.; Oscarson, S.; Roy, R.; King, S.; Kaplan, M. H.; Goldstein, I. J.; Tarbet, E. B.; Hurst, B. L.; Smee, D. F.; de la Fuente, C.; Hoffmann, H. H.; Xue, Y.; Rice, C. M.; Schols, D.; Garcia, J. V.; Stuckey, J. A.; Gabius, H. J.; Al-Hashimi, H. M.; Markovitz, D. M. Engineering a therapeutic lectin by uncoupling mitogenicity from antiviral activity. *Cell* **2015**, *163* (3), 746–58.

(41) Helferty, M.; Vachon, J.; Tarasuk, J.; Rodin, R.; Spika, J.; Pelletier, L. Incidence of hospital admissions and severe outcomes during the first and second waves of pandemic (H1N1) 2009. *CMAJ*. **2010**, *182* (18), 1981–7.

(42) Martic, J.; Savic, N.; Minic, P.; Pasic, S.; Nedeljkovic, J.; Jankovic, B. Novel H1N1 influenza in neonates: from mild to fatal disease. *J. Perinatol.* **2011**, *31* (6), 446–8.

(43) Halasa, N. B. Update on the 2009 pandemic influenza A H1N1 in children. *Curr. Opin. Pediatr.* **2010**, *22* (1), 83–7.